Deposit models for tube support plate flow blockage in Steam Generators

Thomas Prusek, Edgar Moleiro, Fadila Oukacine, André Adobes, Marc Jaeger, Marc Grandotto

Deposit models for tube support plate flow blockage in Steam Generators

T. Prusek [a,*], E. Moleiro [a,**], F. Oukacine [a,**], A. Adobes [a], M. Jaeger [b], M. Grandotto [c]

[a] *Fluid Dynamics, Power Generation and Environment, EDF R&D, 6 quai Watier, Chatou 78401, France*
[b] *École Centrale Marseille, M2P2, CNRS UMR7340, Technopôle de Château-Gombert, 38 rue Frédéric Joliot-Curie, Marseille 13451, France*
[c] *CEA Cadarache, Saint Paul lez Durance 13108, France*

Corrosion product deposits in the secondary side of nuclear power plant Steam Generators may result in Tube Support Plate flow blockage, and tube fouling. In order to simulate those two phenomena in the whole Steam Generator, a solid deposit growth model has been developed by the EDF R&D Division. This model is implemented in the frame of THYC, which is the EDF's reference code for the modeling of two-phase thermal-hydraulic phenomena at the subchannel scale. A new deposit process, based on Tube Support Plate flow blockage studies, has been developed and implemented in the model, and is presented in this work. It can be defined by two main steps: particle deposition, and strengthening process called "flashing" due to soluble species precipitation in the pores of the particle deposit. The relevance of this process is tested by comparing the simulation results to the actual levels of flow blockage observed in some nuclear plants. Two dominant trends are showed in this work: the flow blockage is more important on the hot leg than on the cold leg and at the top than at the bottom of the Steam Generators. Moreover the flow blockages at the upper Tube Support Plate have the special feature to be more important at the periphery than at the center. The "flashing" phenomenon allows one to underline the magnetite solubility dependence, so the pH dependence, of flow blockage phenomenon. A pH elevation of the secondary circuit seems to be a interesting remedy which is currently considered on EDF fleet.

1. Introduction

EDF nowadays operates 58 Pressurized Water Reactors (PWR) which represent more than sixty-three thousand megawatts of installed power capacity and more than 85% of electricity produced in France. Safety and performance of these reactors are crucial targets to ensure electrical supply to the whole national territory. Steam Generators (SG) play a crucial role in this domain both as a safety barrier and as a heat exchanger from the primary to the secondary flow (Fig. 1).

Each Steam Generator contains a high number of thin tubes, between 3000 and 6000. The primary flow, which circulates inside the tubes, comes from the nuclear reactor core. It is maintained at a very high pressure in order to avoid boiling phenomena. The secondary flow, which circulates outside the tubes through the bundle, boils and evaporates in order to produce steam and so electricity. The tubes are supported by several Tube Support Plates (TSP) placed along the tube bundle. Flow holes allow to let the secondary flow go through these Tube Support Plates. Separators located at the top of Steam Generators separate the remaining liquid phase from the steam phase. A Steam Generator is divided in two legs: the hot leg and the cold leg. The primary flow is going up in hot leg, while it is going down in cold leg.

* Corresponding author. Tel.: +33 1 30 87 79 99.
** Corresponding authors.
E-mail addresses: thomas.prusek@edf.fr, thomas.prusek@gmail.com (T. Prusek), edgar.moleiro@edf.fr (E. Moleiro), fadila.oukacine@edf.fr (F. Oukacine), andre.adobes@edf.fr (A. Adobes), marc.jaeger@centrale-marseille.fr (M. Jaeger), marc.grandotto@cea.fr (M. Grandotto).

Nomenclature

Latin

a_v	unobservable parameter
C	mass quality
d_p	diameter of particles (m)
H_{lg}	latent heat of vaporization (J/kg)
J_h	convective and diffusive term of species h (kg/s/m^2)
K	deposition rate (m/s)
k_v	variable blockage rate (1/m)
L	half the distance between two consecutive tubes (m)
m_d	deposited mass per unit surface area (kg/m^2)
M_c	flow blockage mass in one flow hole (kg)
N	total number of deposition iteration
N_{τ_c}	total number of observed rates
P_h	volume mixture transfer between soluble species and particles (kg/m^3/s)
Q_h	volume mixture transfer between species h and boundary wall (kg/m^3/s)
R	flow hole equivalent radius (m)
S	flow hole section (m^2)
S_c	wall surface in contact with flow blockage deposit (m^2)
t	time (s)
T	total time of deposition (s)
U_i	reference inlet velocity (m/s)
U_z	vertical mixture velocity (m/s)
V_c	blockage volume in one flow hole (m^3)

Greek

α	constant = 1.0166
β	constant = 0.023 $\times 10^9$ (m^{-3})
ΔH_l	enthalpy reduction of liquid (J/kg)
ΔH_l^*	dimensionless enthalpy reduction of liquid
Δt	time step of deposition (s)
ε	fluid porosity
ε_c	Tube Support Plate flow blockage deposit porosity
ε_p	particle deposit porosity
Φ	mass flux per unit area (kg/s/m^2)
Γ_h	mass fraction in liquid of species h (kg/kg)
Γ_s^{max}	solubility of soluble species (kg/kg)
η	mass ratio
μ	dynamic viscosity (kg/m/s)
ρ	density (kg/m^3)
τ_c	Tube Support Plate flow blockage rate

Subscripts

c	Tube Support Plate flow blockage deposit
d	deposition
f	fouling deposit
g	steam
h	species (particle or soluble species)
l	liquid
m	mixture
p	particle
r	removal
s	soluble species

Superscripts

I	iteration number of the inverse method
j	control volume number

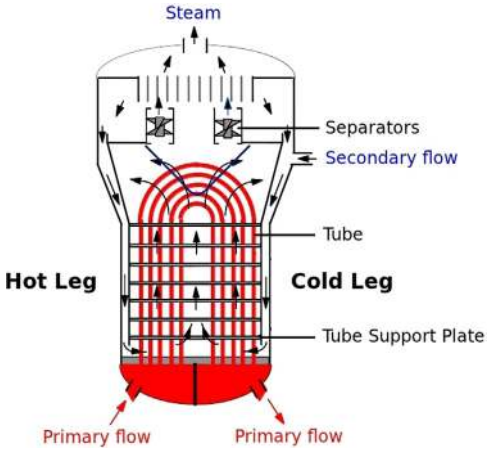

Fig. 1. Schematic view of a Steam Generator.

Corrosion and degradation phenomena of some components and drain systems occur in the secondary circuit of Pressurized Water Reactors. They induce the production and the circulation of corrosion products such as metallic oxides in the secondary flow. Moreover impurities and contaminants from make-up water, auxiliary feed-water and condenser leaks, also circulate in the secondary flow. All those materials are made up of particles and soluble species which can be transported by the liquid phase of the secondary flow to the Steam Generator. As they cannot be transported out of the Steam Generator by the steam phase, those materials remain inside and produce deposits (Corredera et al., 2008).

These deposits have been observed by different control techniques after a working period of Steam Generators. In this work the working period of the considered Steam Generator is equal to 22 years. One of these techniques is called TeleVision (TV) Inspection. A camera is inserted at the top of the Steam Generators and allows to visualize reliably deposits. The advantage of this technique is to precisely determine local deposits with small uncertainties. However it cannot be used all over the Steam Generators because the controls do not reach certain places due to the presence of a compact tube bundle. Although other techniques like Eddy Currents allow one to estimate deposits in most locations of Steam Generators, they are not taken into account in this work because the associated uncertainties are much larger.

Thanks to TV Inspections two main different types of deposits have been found according to their location in Steam Generators and their impact: tube fouling and Tube Support Plate flow blockage. These deposits are supposed to be responsible for different detrimental effects which affect the behavior and the efficiency of Steam Generators.

Tube fouling is a deposit on the tube surfaces as shown in Fig. 2. This deposit phenomenon is penalizing for the heat exchanges between the primary and the secondary circuits (Demasles et al., 2006; Varrin, 2010). Indeed the total thermal resistance between the primary and the secondary flows increase due to the presence of deposits. Tube fouling can also induce a decrease in outlet steam pressure and a loss of efficiency of Steam Generators.

Another detrimental effect is associated with Tube Support Plate flow blockage (Klimas and Turner, 2009; Turner and Klimas, 2008). As shown in Fig. 3, Tube Support Plate flow blockage is a deposit at the inlet of Tube Support Plate flow holes. This deposit phenomenon can induce high velocity zones and transverse velocities in the secondary flow, then flow induced vibrations and tube cracks in some cases. Indeed three significant primary to secondary leaks occurred at one nuclear plant in France between 2004 and 2006. The thermal-hydraulic and vibration studies confirmed a cracking mechanism caused by flow induced vibrations resulting in a circumferential

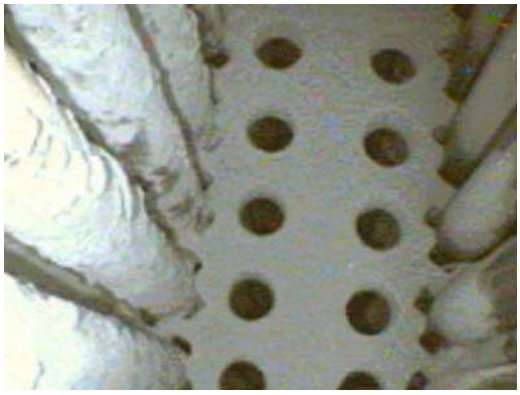

Fig. 2. Photo of tube fouling: hot leg on the left side and cold leg on the right side.

crack. Those studies pointed out the role of an important flow blockage distribution at the upper Tube Support Plate as an aggravating factor.

In this context, this work describes the efforts performed by the EDF R&D Division to specify and implement a model for the growth of solid deposits on the secondary side of Steam Generators, and more specifically on their Tube Support Plates. This deposit model has been implemented in the frame of EDF thermal-hydraulic reference code called THYC. This model aims to predict the localization and the growth rate of deposits in order to simulate tube fouling as well as Tube Support Plate flow blockage.

THYC is a three dimensional thermal-hydraulic code, which allows one to simulate two-phase flows and heat exchanges at the subchannel scale for industrial heat exchangers (David, 1999). A subchannel scale is a mesoscale which has the advantage to calculate thermal-hydraulic flows in whole nuclear components with reasonable CPU times. THYC is applicable to different kinds of heat exchangers: single-phase heat exchangers, condensers and Steam Generators. It is used to improve the performances and guarantee the safety of Pressurized Water Reactors. Coupled with a deposit model, it provides the frame to simulate deposition. Indeed it allows one to access all the required thermal-hydraulic data which are necessary to calculate the growth of deposits.

Based on a porous media approach, the THYC model is obtained by using a space–time averaging of the instantaneous equations: mass, momentum and energy. In the Steam Generator case, it solves these three conservation equations for the fluid mixture outside the tubes (secondary flow). Actually the liquid and steam phases are considered to be one fluid which is an homogeneous mixture. These equations are also coupled with an energy equation of the fluid inside the tubes (primary flow). A Finite Volume method on a regular staggered grid is used to solve these equations. Each control volume includes fluid and solids. A fluid porosity term ε is used in the equations to represent the ratio between the fluid volume V and the total volume V_t.

$$\varepsilon = \frac{V}{V_t} \tag{1}$$

In order to simulate the fouling and flow blockage phenomena in the whole Steam Generator, one of the solutions developed at EDF is to perform fundamental studies and numerical simulations at the subchannel scale. On the basis of the thermal-hydraulic data from THYC, a model of tube fouling had been previously developed (Pujet et al., 2004). An extension of this model has been implemented in order to specifically simulate Tube Support Plate flow blockage (Moleiro et al., 2010).

A new deposit process for the Tube Support Plate flow blockage phenomenon has been developed and implemented in the model, and is presented in this work. It can be defined by two main steps: particle deposition, and strengthening process called "flashing" due to soluble species precipitation in the pores of the particle deposit. The relevance of this process is tested by comparing the simulation results to the actual levels of flow blockage observed in some nuclear plants. A sensitivity analysis of soluble species solubility, and more specifically magnetite solubility, has been also performed.

2. The deposit model

2.1. General equations

The deposit model has been developed to estimate iron oxide deposits on tubes and Tube Support Plates (Moleiro et al., 2010; EPRI, 2007). These species are introduced in the Steam Generator by feed-water, transported by the secondary flow, deposited on the surfaces, and can be removed by the flow. The model assumes that there is one layer of magnetite deposit with a given porosity denoted ε_f for tube fouling and ε_c for Tube Support Plate flow blockage. These porosities are different from the fluid porosity which is introduced in THYC and used in Eq. (2). Actually the deposit can also be made up of minority species such as copper, and the porosity of the deposit is not uniform. The deposit masses are created both by particle deposition and by soluble species precipitation into the pores of the deposits. These masses are calculated as a function of time and space in the secondary circuit of Steam Generators by two coupled equations:

$$\frac{\partial}{\partial t}(\varepsilon \rho_m C_l \Gamma_h) + \vec{\nabla}.(J_h) = P_h + Q_h \tag{2}$$

Fig. 3. Photo of Tube Support Plate flow blockage: top view of a "clean" flow hole on the left side and an entirely blocked flow hole on the right side (tube on the right side).

$$\frac{dm_d}{dt} = \sum_{h\in\{p,s\}} \Phi_{d,h} - \Phi_r \quad (3)$$

Eq. (2) is a transport equation (Pascal-Ribot et al., 1997; Liner et al., 1990) which allows one to determine the value of the mass fraction Γ_h of species h in liquid phase. These species correspond to both suspended particles ($h=p$) and soluble species ($h=s$). On the left side of Eq. (2), the transient term accounts for the accumulation of the quantity $\varepsilon\rho_m C_l \Gamma_h$ where ρ_m and C_l are respectively the density of the homogeneous mixture and the mass quality of liquid. This quantity represents the mass concentration of each species in liquid for each control volume. In this equation the volumetric units refer to volume mixture. The second term on the left side of this equation is a transport term by convection and diffusion of the mass concentration. This transport is due to the presence of both liquid velocity and mass fraction gradient. On the right side of this equation, Q_h and P_h are the source terms which either create or destroy this quantity, depending of their signs. The term Q_h represents the volume mixture transfer between the species h and the boundary wall. It corresponds to deposition of species h on walls or removal of deposits. The term P_h represents the volume mixture transfer between the soluble species and the particles. It corresponds to precipitation of soluble species or dissolution of particles. In the deposit model, the dissolution of particles is neglected and the precipitation of soluble species is supposed to instantaneously create particles with a single size denoted d_p.

Eq. (3) is a growth equation of deposit masses on the boundary wall. For each deposit phenomenon: tube fouling ($d=f$) or Tube Support Plate flow blockage ($d=c=$), it allows one to calculate the masses m_d deposited per unit surface area from the material fluxes of particle deposition and soluble species precipitation, denoted $\Phi_{d,p}$ and $\Phi_{d,s}$, and the flux Φ_r of removed deposits. These fluxes are determined by specific empirical correlations based on literature. In this work, the flux Φ_r is not taken into account ($\Phi_r = 0$). The fluxes $\Phi_{d,p}$ and $\Phi_{d,s}$ depend on the mass fraction of each species in liquid which is calculated by the transport equation. They also depend on a combination of thermal-hydraulic parameters calculated by THYC. For the tube fouling phenomenon, the fluxes $\Phi_{f,p}$ and $\Phi_{f,s}$ seem to be properly described by the overall effect of the following classical deposit mechanisms: diffusion, turbulent inertia, thermophoresis, sedimentation due to gravity, and deposition or precipitation associated with boiling (Beal and Chen, 1986; Liner et al., 1992; Turner et al., 1994). For the Tube Support Plate flow blockage phenomenon, the fluxes $\Phi_{c,p}$ and $\Phi_{c,s}$ can be described by other deposit mechanisms which are detailed in this work.

2.2. Tube Support Plate flow blockage model

The deposit model, based on Tube Support Plate flow blockage studies (Rummens, 1999; Rummens et al., 2004), can be defined by two main steps: particle deposition, and strengthening process called "flashing" due to soluble species precipitation in the pores of the particle deposit.

2.2.1. Particle deposition

The "lipping" phenomenon observed at the inlet of flow holes shown in Fig. 3 can be attributed to the presence of a sudden contraction. In this work, this contraction is also called vena contracta. A conceptual figure of a vena contracta is shown in Fig. 4. This figure does not represent exactly the real geometry of a flow hole. It just allows one to describe the main hydraulic mechanisms when a flow passes through the contraction. At the inlet of the vena contracta, the mainstream flow separates from the wall following the sharp contraction. A low-velocity recirculation zone is created beside the support. In this zone, the particle deposition is encouraged and

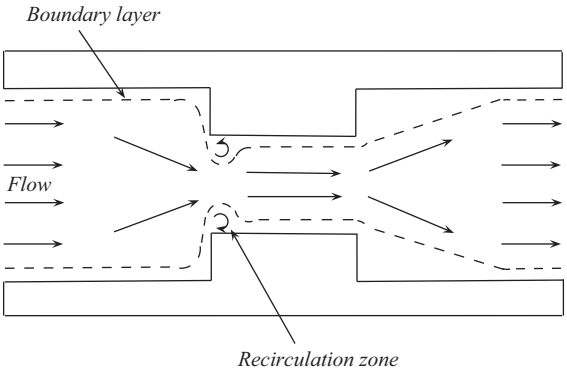

Fig. 4. Pattern of vena contracta region.

a tiny deposit can begin to grow. As the deposit grows, the flow contraction and associated boundary-layer separation will become more severe. The particle deposition is more and more encouraged, so this vena contracta mechanism tends to become progressively worse.

The flux of particle deposition $\Phi_{c,p}$ is considered to be exclusively caused by this vena contracta mechanism, and to be equal to the flux of particles transported to the wall. In other words, it is assumed that all the particles transported to the wall are deposited on it, leading to the following expression for $\Phi_{c,p}$:

$$\Phi_{c,p} = K_{c,p}\rho_m C_l \Gamma_p \quad (4)$$

Where a deposition rate $K_{c,p}$ is used to model the vena contracta mechanism (Prusek et al., 2011). It takes into account the main parameters which seem to influence Tube Support Plate flow blockage such as mass quality of vapor C_g and vertical fluid velocity U_z:

$$K_{c,p} = a_v \frac{k_v(\rho_p - \rho_l)U_z^2 C_g d_p^2}{\mu_l} \quad (5)$$

As the density ρ_p of particles is higher than the density ρ_l of liquid, the positive term $\rho_p - \rho_l$ represent an inertial term for the particles. The higher the density of particles is, the more the particle deposition and the associated deposition rate increase. The term U_z^2 is proportional to a kinetic energy for the d_p-size particles. The higher this energy is, the more the deposition rate increases. The dynamic viscosity μ_l of liquid allows one to take into account the viscous forces induced by the flow. These forces can be a factor which removes a part of deposits and limits the particle deposition. The more important the value of viscosity is, the more the viscous forces increase, and the more the deposition rate decreases. Parameter k_v allows to take into account that the Tube Support Plate flow blockage phenomenon self-sustained and can even accelerate and become progressively worse. This parameter is modeled by the following expression:

$$k_v = \frac{L - [R(1-\tau_c)]}{S} \quad (6)$$

Where the constants L, R and S are characteristic values of the specific geometry of flow holes. They respectively represent half the distance between two consecutive tubes, the equivalent radius of a flow hole and its section, as shown in Fig. 5. The validity domain of this correlation is limited to "classical" flow holes, which means quasi-spherical flow holes with an equivalent radius lower than half the distance between two consecutive tubes.

In this correlation, parameter τ_c represents the Tube Support Plate flow blockage rate which is a ratio between the flow blockage section to the total hole section. It is a dimensionless number and its value varies from 0 to 1. A value equal to 0 means that there is no blockage deposit in the flow hole, and a value equal to 1 means that

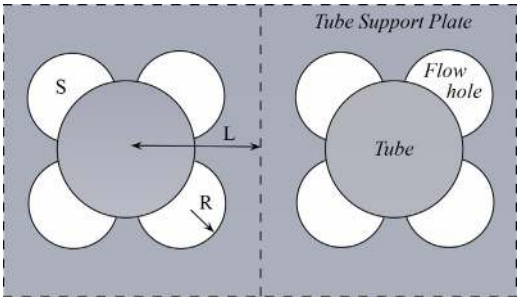

Fig. 5. Top view of a pattern of a Tube Support Plate (solid in gray color and secondary flow in white color).

the flow hole is entirely blocked. The calculation of this blockage rate is obtained thanks to a specific correlation established from Steam Generators experience data (Moleiro et al., 2010). This correlation (7) allows one to determine the blockage rate of each flow hole from the volume V_c of the deposited mass in each flow hole which is calculated by the deposit model:

$$\tau_c = \alpha(1 - e^{-\beta V_c}) \tag{7}$$

where α and β are determined constants. Their values are respectively 1.0166 and $0.023 \times 10^9\ \mathrm{m}^{-3}$. The validity domain of this correlation is for deposited volumes included between 0 mm^3 and 178,91 mm^3.

Eq. (6) shows that the more important the blockage rate is, the more parameter k_v and so the deposition rate of vena contracta increase. This is consistent with the fact that the vena contracta mechanism tends to become more and more important as the blockage rate increases.

In Eq. (5), we can see that the deposition rate also depends on an unobservable parameter denoted a_v. This parameter is supposed to be constant all over the Steam Generator. It allows one to calibrate the deposition rate. It could be determined by specific experiments performed on devoted test-facilities but at the Steam Generator Scale and in Pressurized Water Reactors conditions, its value is not determined. In this work, an inverse method (Tarantola, 1994) has been developed in order to determine a value for this unobservable parameter. This method could enable one to evaluate a likely value by fitting the results of deposit simulations to the actual levels of Tube Support Plate flow blockage rates observed in some French nuclear plants. More details of this method are given in Section 3.

2.2.2. Soluble species precipitation

The precipitation of soluble species can be attributed to a sudden pressure reduction which is created at the inlet of flow holes due to the presence of the sharp contraction (Fig. 4). This pressure reduction can be linked to an enthalpy reduction which may induce a local liquid to steam change. Due to this vaporization, the mass fraction of soluble species in liquid locally increases as they cannot be transported by the steam phase. If this increase is high enough to exceed the limit of solubility, a local precipitation of soluble species occurs. The solubility represents the maximum mass fraction of soluble species which is possible to have in liquid. In this work, we supposed that the limit of solubility has to be reached in order to generate precipitation. Due to this phenomenon called flashing mechanism, a precipitated mass can also be created at the inlet of flow holes. This mass may act as a deposit cementing agent and strengthen a preliminary particle deposit.

The flux of soluble species precipitation $\Phi_{c,s}$ is considered to be exclusively caused by this flashing mechanism. In the deposit model, the soluble species are supposed to be at saturation. It means that their mass fraction is equal to the solubility denoted Γ_s^{max} in the whole secondary flow of Steam Generators. This hypothesis

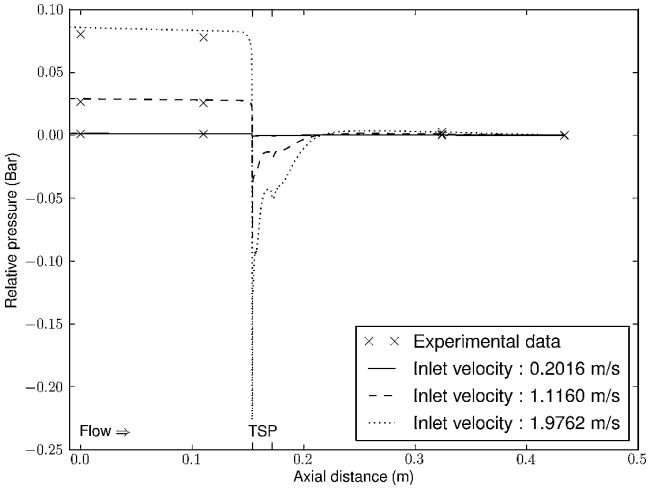

Fig. 6. Axial pressure loss profiles through Tube Support Plate with 0% blockage rate.

allows one to maximize the flashing mechanism. In other words, all the soluble species, initially included in the liquid which vaporizes, precipitate. All this precipitated mass is supposed to strengthen the particle deposit. By denoting Φ_g the mass flux of steam created at the inlet of a flow hole due to the flashing mechanism, the flux $\Phi_{c,s}$ is easily given by the following expression:

$$\Phi_{c,s} = \Phi_g \Gamma_s^{max} \tag{8}$$

In this work the steam enthalpy is supposed to be fairly insensitive to pressure and we use the notation H_{lg} for the latent heat of vaporization. The increase of created steam mass flux can be expressed as a function of the mass flux of liquid Φ_l and the enthalpy reduction ΔH_l of liquid at the inlet of the flow hole (Rummens, 1999):

$$\Phi_g = \Phi_l \frac{\Delta H_l}{H_{lg}} \tag{9}$$

The mass flux of liquid and the latent heat of vaporization are calculated by the THYC code. However the local and sudden enthalpy reduction of liquid cannot be captured at the subchannel scale by this code. In order to quantify a estimate for this variable, CFD calculations on a realistic geometry of flow holes have been performed with *Code_Saturne*. *Code_Saturne* is an open-source CFD code which has been developed by EDF (Archambeau et al., 2004). In this work, the calculations were performed in single phase flow conditions and for different typical geometries of Tube Support Plate flow blockage rates. The R_{ij}-ε *LRR* URANS turbulence model, which is implemented in *Code_Saturne*, was used to simulate the flow. Constant and uniform velocity profiles denoted U_i were assumed as inlet boundary condition downstream from the flow hole. As the variables of interest in these calculations are pressure or enthalpy drops, a zero pressure was imposed as the outlet boundary condition upstream from the flow hole.

The calculated axial pressure loss profiles through Tube Support Plate with 0% blockage rate and for different inlet liquid velocities along a vertical line are shown in Fig. 6. This line goes through the minimum calculated pressure point at the inlet of the flow hole in the near wall area. The results of these calculations have been compared to experimental results. These experimental results have allowed to estimate the total pressure losses induced by different Tube Support Plate flow blockage rates in single phase flows (Brunin et al., 2010). They are represented by crosses in Fig. 6. The total pressure losses through Tube Support Plate with 0% blockage rate is well estimated by CFD calculations for each tested inlet velocity in comparison with the measured total pressure losses. The

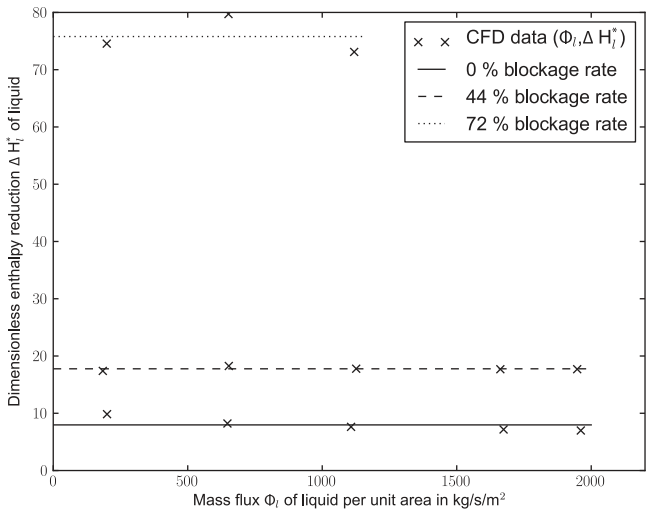

Fig. 7. Correlation between mass flux and dimensionless enthalpy reduction of liquid.

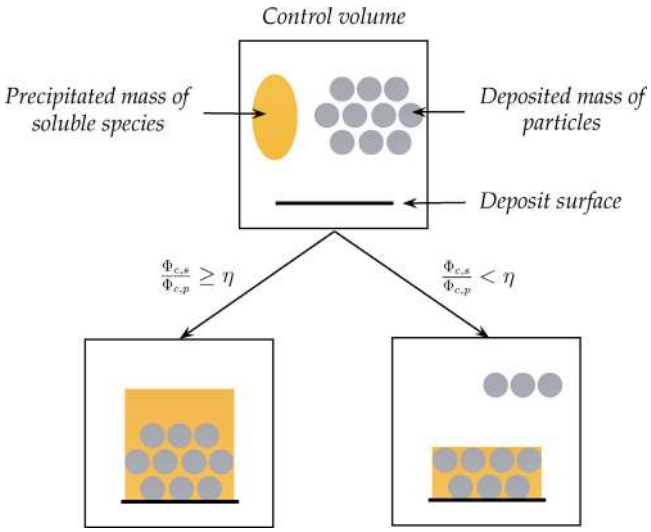

Fig. 8. Principle of the strengthening process implemented in the deposit model.

relative errors between measured and calculated relative pressures are included between 10% and 20%. Other CFD calculations of two configurations corresponding to 44% and 72% blockage rates have been also performed. They are not presented in this work but they showed such satisfactory results.

The advantage of these CFD calculations is to capture the sudden and local pressure reduction at the inlet of Tube Support Plates in the near wall area due to the flow hole contraction, as shown in Fig. 6. The enthalpy reduction was deduced from this pressure reduction thanks to the thermal-hydraulic tables. A dimensionless enthalpy reduction ΔH_l^* is then defined at the inlet of Tube Support Plates from this enthalpy reduction and a reference inlet velocity by the following expression:

$$\Delta H_l^* = \frac{\Delta H_l}{U_i^2} \tag{10}$$

As shown in Fig. 7, the mass flux of fluid at the inlet of Tube Support Plates does not seem to have a strong impact on dimensionless enthalpy drop except for the 72% blockage rate. For each blockage rate, the dimensionless enthalpy drop at the inlet of Tube Support Plates obtained from CFD results is thus supposed to be independent of the mass flux:

$$\Delta H_l^* = \lambda(\tau_c) \tag{11}$$

In this work, an approximation is made in order to simplify the flashing mechanism. The value of λ is supposed to be independent of the blockage rate and equal to the value for the case without blockage deposit:

$$\lambda = 7.97 \tag{12}$$

2.2.3. Strengthening process of deposits

After a working period of Steam Generators, the blockage deposits have been precisely determined at the upper Tube Support Plate by using a technique of TV Inspection. This technique cannot be used for any other Tube Support Plates because the controls do not reach those places. During this control period, very hard deposits have been found in the flow holes. These deposits cannot be removed easily from Tube Support Plates. Their porosity denoted ε_c was estimated at a very low value approximately equal to 0.05.

A strengthening process called "flashing" due to a combination of two steps may explain such compact deposits: firstly a preliminary particle deposit with a porosity ε_p which is higher than ε_c, and secondly a strengthening process due to soluble species precipitation in the pores of this particle deposit. A ratio η between the volume V_s of precipitated soluble species and the volume V_p of deposited particles which allows to reach a deposit with a porosity equal to ε_c is defined by the following expression:

$$\eta = \frac{V_s}{V_p} \tag{13}$$

By using the porosity definition, this ratio can be expressed as a function of the porosities ε_c and ε_p:

$$\eta = \frac{1-\varepsilon_c}{1-\varepsilon_p} - 1 \tag{14}$$

In this work, the particles are supposed to be spherical with a single size. The highest density, that is the greatest fraction of space occupied by such particles in order to have a deposit as dense as possible, is obtained by the face-centered cubic arrangement. This arrangement leads to a compacity approximately equal to 0.74. For that reason, the porosity ε_p of preliminary particle deposit is supposed to be equal to $1 - 0.74 = 0.26$ in the deposit simulations. In such a case, the ratio η is equal to 0.28. It means that a precipitated volume of soluble species equal to 28% of the deposited volume of particles is needed in order to strengthen the preliminary particle deposit and obtain a porosity equal to ε_c.

Fig. 8 shows the principle of the strengthening process implemented in the deposit model. It is based on the hypothesis that the deposited mass of particles needs a minimum precipitated mass of soluble species in order to strengthen and generate deposits. However the precipitated mass of soluble species can deposit without the presence of a deposited mass of particles.

The masses of deposited particles and precipitated soluble species are also compared. Two different cases can be defined from the values of the flux $\Phi_{c,s}$ of precipitated soluble species and the flux $\Phi_{c,p}$ of deposited particles respectively determined by Eqs. (4) and (8), and the ratio η calculated by Eq. (14):

- if $(\Phi_{c,s}/\Phi_{c,p}) \geq \eta$, the precipitated mass of soluble species is high enough to strengthen the whole particle deposit. Therefore the fluxes are not changed and all particles and soluble species deposit. Even if the precipitated mass of soluble species is more important than the one which is necessary to strengthen the particle deposit, the possible excess of precipitation is also supposed to deposit.

- if $(\Phi_{c,s}/\Phi_{c,p}) < \eta$, the precipitated mass of soluble species is not high enough to strengthen the whole particle deposit. In such a case, only the part of particles, which can be strengthened by soluble species precipitation, deposits. Therefore the flux of particle deposition is limited by Eq. (15). The remaining part of particles keeps circulating in the secondary flow of Steam Generators.

$$\Phi_{c,p} = \frac{\Phi_{c,s}}{\eta} \tag{15}$$

3. The inverse method

In this work, an inverse method has been developed to calibrate the deposit model by fitting the results of it to the actual levels of Tube Support Plate flow blockage observed in some French nuclear plants (Prusek et al., 2011). This inverse method aims to evaluate an optimum value of the unobservable parameter a_v which allows to calibrate the vena contracta mechanism.

3.1. Mathematical formulation of the inverse method

In control volume denoted j the flux of particle deposition is described by an equation of the form of Eq. (16). The term $\Psi^j_{c,p}$ is a set of thermal-hydraulic or chemical parameters which are computed from the THYC code and the deposit model: Eqs. (4) and (5). This equation depends on the unobservable parameter denoted a_v that we would like to evaluate.

$$\Phi^j_{c,p} = a_v \Psi^j_{c,p} \tag{16}$$

At the final time of deposition denoted T the Tube Support Plate flow blockage rate $\tau_c(T)$ in control volume j can be written as an integral from the initial time $t=0$ to the final time $t=T$ by considering no blockage rate at the initial time.

$$\tau^j_c(T) = \int_{t=0}^{t=T} \frac{\mathrm{d}\tau^j_c}{\mathrm{d}t}\,\mathrm{d}t \tag{17}$$

This integral can be expressed as a sum of integrals according to the time step of deposition Δt (=10 days in the calculations) and the total number of iteration N by considering $T = N\Delta t$:

$$\int_{t=0}^{t=T} \frac{\mathrm{d}\tau^j_c}{\mathrm{d}t}\,\mathrm{d}t = \sum_{n=1}^{N} \left(\int_{t=(n-1)\Delta t}^{t=n\Delta t} \frac{\mathrm{d}\tau^j_c}{\mathrm{d}t}\,\mathrm{d}t \right) \tag{18}$$

Each integral from $t_{n-1} = (n-1)\Delta t$ to $t_n = n\Delta t$ can be linearly approximated by the following discrete sum. The error of this approximation is in the 1st order.

$$\int_{t_{n-1}}^{t_n} \frac{\mathrm{d}\tau^j_c}{\mathrm{d}t}\,\mathrm{d}t \approx \frac{\Delta t}{2}\left[\frac{\mathrm{d}\tau^j_c}{\mathrm{d}t}(t_{n-1}) + \frac{\mathrm{d}\tau^j_c}{\mathrm{d}t}(t_n) \right] \tag{19}$$

The derivative of Tube Support Plate flow blockage rate with respect to time is obtained from Eq. (7):

$$\frac{\mathrm{d}\tau^j_c}{\mathrm{d}t} = \alpha\beta \frac{\mathrm{d}V^j_c}{\mathrm{d}t} e^{-\beta V^j_c} \tag{20}$$

The volume of Tube Support Plate flow blockage deposit V^j_c in one flow hole is calculated from its mass M^j_c, its porosity ε_c (=0.05) and the density of particles ρ_p (=5200 kg/m^3).

$$V^j_c = \frac{M^j_c}{(1-\varepsilon_c)\rho_p} \tag{21}$$

Where M^j_c is linked to the deposited mass per unit surface area m^j_c in control volume j and the wall contact surface with flow blockage deposit S_c.

$$M^j_c = S_c m^j_c \tag{22}$$

The derivative of V^j_c with respect to time is calculated from Eqs. (21) and (22) by considering ε_c, ρ_p and S_c to be constant.

$$\frac{\mathrm{d}V^j_c}{\mathrm{d}t} = \frac{S_c}{(1-\varepsilon_c)\rho_p} \frac{\mathrm{d}m^j_c}{\mathrm{d}t} \tag{23}$$

The value of the derivative of deposited mass per unit surface area with respect to time is calculated from Eqs. (3) and (16):

$$\frac{\mathrm{d}m^j_c}{\mathrm{d}t} = a_v \Psi^j_{c,p} + \Phi^j_{c,s} \tag{24}$$

The mass fraction Γ^j_p and Γ^j_s and the deposited mass per unit surface area m^j_c are respectively determined by solving Eqs. (2) and (3). The main problem is that these equations depend on the unknown value of a_v. Let a^I_v be the value of a_v calculated by the inverse method at the iteration I. The objective is to determine a^{I+1}_v. We consider that the mass fraction $\Gamma^{j,I}_p$ and $\Gamma^{j,I}_s$ and the deposited mass per unit surface area $m^{j,I}_c$ are calculated from Eqs. (2) and (3) where a_v is equal to a^I_v. The Tube Support Plate flow blockage rate at the final time can be also written with the following numerical scheme from Eqs. (17)–(24):

$$\tau^j_c(T) = a^{I+1}_v \Theta^{j,I}_{c,p}(T) + \Theta^{j,I}_{c,s}(T) \tag{25}$$

Where $\Theta^{j,I}_{q\in\{(c,p),(c,s)\}}$ has the following expression at the iteration I:

$$\Theta^{j,I}_q(T) = C \sum_{n=1}^{N} [f^{j,I}_q(t_{n-1}) + f^{j,I}_q(t_n)] \tag{26}$$

Where

$$C = \frac{\alpha\beta S_c \Delta t}{2(1-\varepsilon_c)\rho_p} \tag{27}$$

And

$$f^{j,I}_{c,p}(t) = \Psi^{j,I}_{c,p}(t)\, e^{-\beta V^{j,I}_c(t)} \tag{28}$$

$$f^{j,I}_{c,s}(t) = \Phi^{j,I}_{c,s}(t)\, e^{-\beta V^{j,I}_c(t)} \tag{29}$$

By using the notations $[.]_{n_l}$ for a n_l vector and $(.)_{i_l}$ its general term in line i_l, the inverse problem can be expressed as an iterative matrix scheme:

$$[\tau_c]_{N_{\tau_c}} = a^{I+1}_v [A^I]_{N_{\tau_c}} + [B^I]_{N_{\tau_c}} \tag{30}$$

Where N_{τ_c} is the total number of observed rates. $[A^I]$ and $[B^I]$ are totally determined by a combination of known parameters at the iteration I. The general terms of these matrix are detailed below:

$$\forall j \in \{1,\ldots,N_{\tau_c}\},\ (A^I)_j = \Theta^{j,I}_{c,p}(T) \tag{31}$$

$$\forall j \in \{1,\ldots,N_{\tau_c}\},\ (B^I)_j = \Theta^{j,I}_{c,s}(T) \tag{32}$$

The unobservable parameter a^{I+1}_v is calculated by using the least-squares method. We use this method because the system is overdetermined (generally $N_{\tau_c} > 1$): this is a system in which there are more equations than unknowns. The solution a^{I+1}_v is also the optimum solution in the least-squares sense. A convergence criterion is defined to allow the iterative process to stop. This criterion

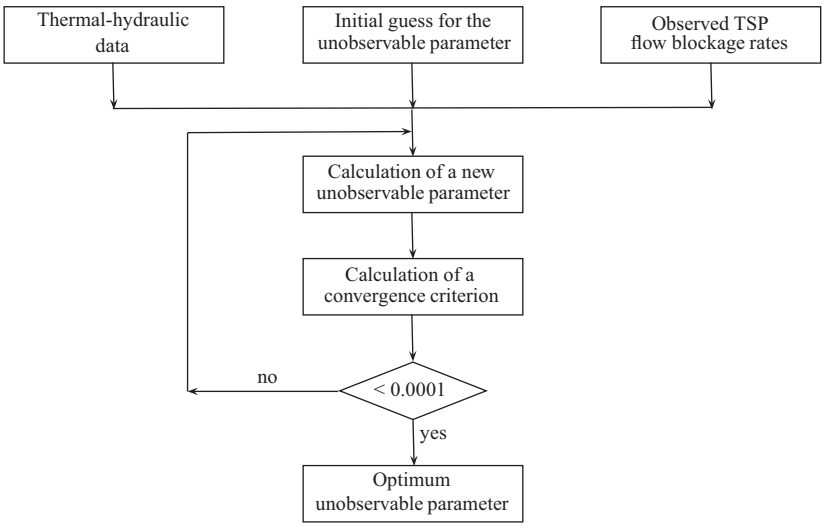

Fig. 9. Inverse method for estimation of the unobservable parameter a_v.

represents the relative variation of the unobservable parameter calculated between two consecutive resolution steps:

$$\frac{|a_v^{I+1} - a_v^I|}{a_v^I} < 10^{-4} \tag{33}$$

3.2. Summary of the inverse method

The main stages of the inverse method are described in Fig. 9. The thermal-hydraulic quantities calculated by the THYC code, an initial guess $a_v^{I=0}$ for the unobservable parameter and $N_{\tau_c} = 422$ local values of blockage rates observed at the upper Tube Support Plate by TV Inspections are the input data of the inverse method. An inverse model calculates a new value of the unobservable parameter a_v^{I+1} at the iteration I which allows an optimum fitting of the observed data. Then a convergence criterion equal to the relative variation between two consecutive calculations of a_v is estimated. If it is higher than 10^{-4}, the process will iterate one more time. Otherwise the process will stop and an optimum value of a_v, which allows to fit the observed data, is found. In other words this optimum value of a_v associated with the deposit model allows one to derive the simulated Tube Support Plate flow blockage rates that are closest to the observed blockage rates.

4. Results

4.1. Influence of the strengthening process

In this section, the deposit simulations have been performed over a period of 22 years. This period corresponds to the working period of the considered Steam Generator before TV Inspections. The Steam Generator is supposed to operate in nominal conditions all over this period. In order to quantify the influence of the strengthening process, two deposit simulations have been tested:

- Simulation 1: only the flux of particle deposition calculated by Eq. (4) due to the presence of vena contracta is taken into account. It means that the strengthening process described in Fig. 8 is not considered. All particles are supposed to deposit and no strengthening process by soluble species precipitation is needed to generate deposits. This is a simplified model. The main goal is to compare the results obtained by Simulation 1 and Simulation 2 in order to quantify the influence of the strengthening process.
- Simulation 2: this time the strengthening process of particle deposit described in Fig. 8 is taken into account. The particles need to be strengthened by soluble species precipitation in order to generate deposits. This is the full model. The fluxes of particles deposition and solubles species precipitation are calculated by Eqs. (4), (8) and (15).

4.1.1. Estimation of the unobservable parameter

Before performing the direct deposit simulations, the vena contracta mechanism is calibrated on the observed blockage rates by using the inverse method. For each simulation and from the initial guess $a_v = 10^{-4}$, the inverse problem is solved until the convergence criterion becomes less than 10^{-4}. The convergence graphs of the unobservable parameter a_v are shown in Fig. 10. For Simulation 1, the inverse method converges after 13 iterations and allows one to evaluate a_v at 0.0008. For Simulation 2, it converges after 17 iterations and allows one to evaluate a_v at 0.00087.

The value of a_v for Simulation 2 is slightly higher than the one for Simulation 1. It may be explained because the strengthening process of deposits seems to be a limiting factor for deposition. Not all the deposited particles can be strengthened because a lack of soluble species precipitation was found in some flow holes of the Steam Generator. Therefore the inverse method mathematically increases

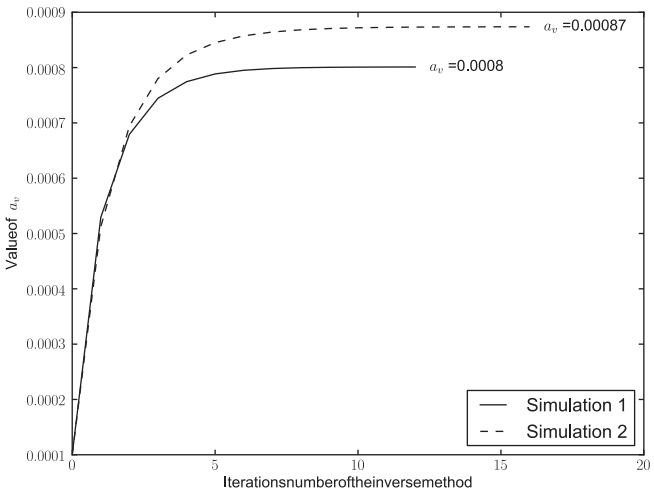

Fig. 10. Convergence graphs of the unobservable parameter a_v.

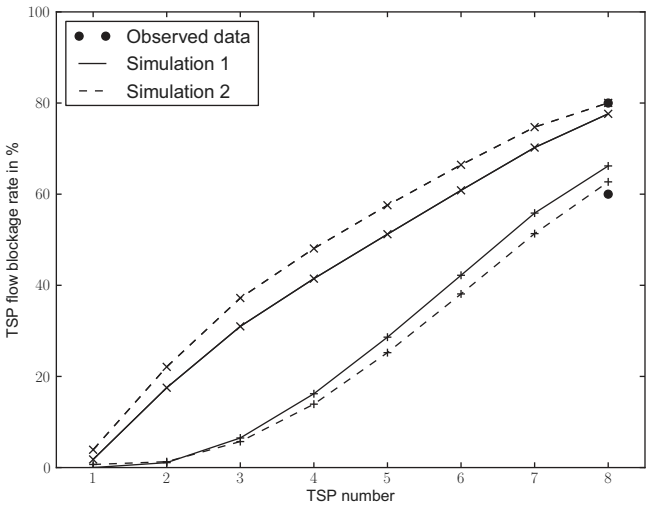

Fig. 11. Profiles of mean flow blockage rates for each Tube Support Plate in hot leg (×) and in cold leg (+) with optimum values of a_v.

the flux of deposited particles by estimating a higher value of a_v. This increase allows to obtain the same order of magnitude for blockage rates in the two simulations, and reach the observed data in Steam Generators.

4.1.2. Direct deposit simulation

The unobservable parameter a_v is now supposed to be known for each simulation. Direct deposit Simulations 1 and 2 were performed over the working period of the considered Steam Generator. The calculated profiles of mean Tube Support Plate flow blockage rates at the end of this period are presented in Fig. 11.

The fitted mechanism allows one to obtain two dominant trends for the Tube Support Plate blockage rates in Steam Generators whatever the simulation. The mean blockage rate of each Tube Support Plate is firstly more important in hot leg than in cold leg. It is secondly more important at the top of the Steam Generator (Tube Support Plates number 5, 6, 7, 8) than at the bottom (Tube Support Plates number 1, 2, 3, 4).

For Simulation 1, the mean blockage rate calculated at the upper Tube Support Plate (Tube Support Plate number 8) in hot leg is close to observed data: the results differ only by 3%. The limit of this simulation is essentially to overestimate the mean blockage rate at the upper Tube Support Plate in cold leg: the results differ by 10%. For Simulation 2, the mean blockage rates calculated at the upper Tube Support Plate are very close to observed data for each leg: the results are less than 1% in hot leg and differ only by 4% in cold leg. Simulation 2 taking into account the strengthening process of deposits allows one to have a better representation of the asymmetry between hot leg and cold leg than Simulation 1 in comparison to observed data.

For Simulation 2, observed and calculated flow blockage rates at the upper Tube Support Plate are compared in Fig. 12 only at the locations where TV Inspections were performed. The relative error between these two distributions is shown in Fig. 13. The relative error is lower than 0.15 for 60.7% of calculated flow blockage rates, lower than 0.30 for 88.9% of them and it is higher than 0.30 only for 11.1% of them. The most important differences come mainly from the cold leg where the flow blockage rates are overestimated. In the hot leg they are globally lower than 30% except for a few control volumes.

For the two simulations, the local flow blockage rates obtained at each Tube Support Plate of the considered Steam Generator are presented in Fig. 14. The Tube Support Plate flow blockage rate distribution between Simulations 1 and 2 are similar. Nevertheless

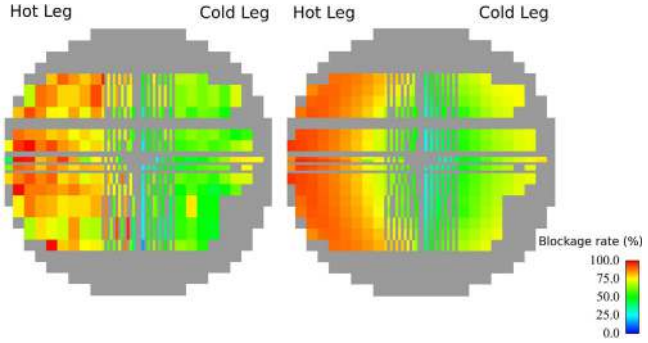

Fig. 12. Comparison between observed (left side) and calculated (right side) flow blockage rates at the upper Tube Support Plate.

Simulation 2 show more important blockage rates in hot leg and lower blockage rates in cold leg than Simulation 1 as it was shown in Fig. 11. These two calculations seem interesting because the distribution of calculated blockage rates at the upper Tube Support Plate has the special feature to be more important at the periphery than at the center. This result is in agreement with observed data in some nuclear plants.

The obtained distributions in this figure show a symmetrical axis at each Tube Support Plate for each leg. This is one of the limits of these two simulations. The calculated flow blockage distributions are necessarily symmetrical with respect to this axis. Actually the deposit mechanisms depend on thermal-hydraulic parameters which are symmetrical with respect to the same axis according to calculations. It is therefore normal to obtain such distributions. However TV Inspections showed that the flow blockage distributions were not symmetrical for the considered Steam Generator. One solution to make the deposit model non symmetrical could be to take into account tube plugging. At some given times of the Steam Generator working, some tubes are plugged for safety reasons. It could have an impact on thermal-hydraulic parameters because no more thermal exchange occurs for these plugged tubes. As tube plugging is not performed in a symmetrical way, its impact could also make thermal-hydraulics, and so deposition, non symmetrical. Another solution would be to take into account the swirl imparted by the liquid/steam separators at the top of Steam Generators (Fig. 1). The velocity of the secondary flow going down to the bottom of Steam Generators is not uniform all around the periphery. Therefore asymmetry could be due to a non symmetrical distribution of transported particles and solubles species at the bottom, then all over the Steam Generators. It could also have a non symmetrical impact on deposition.

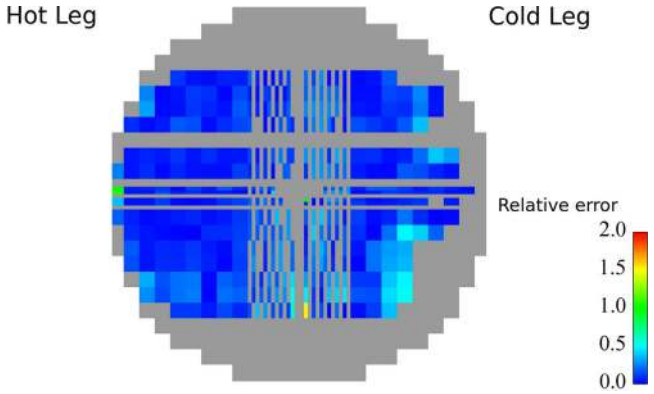

Fig. 13. Relative error between observed and calculated flow blockage rates at the upper Tube Support Plate.

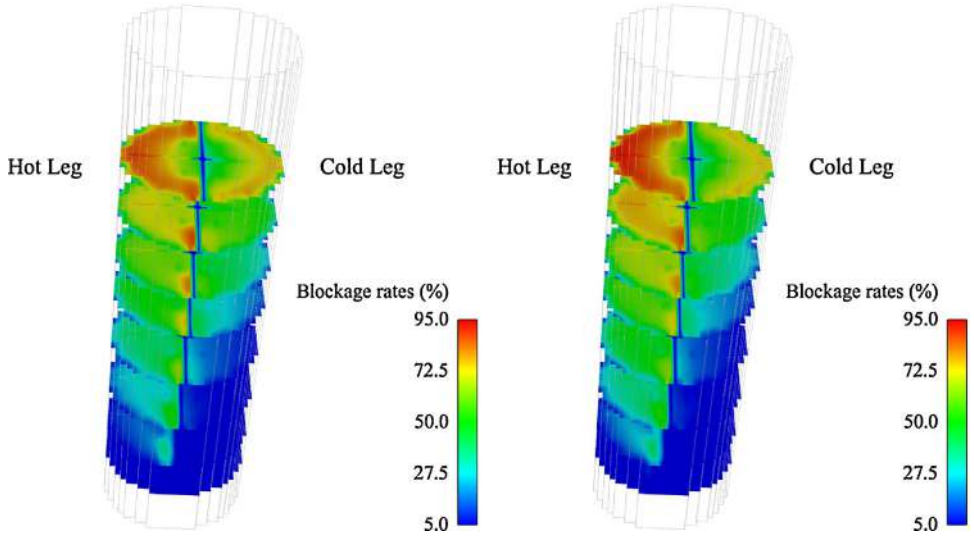

Fig. 14. Distribution of flow blockage rates from the lower to the upper Tube Support Plates for Simulation 1 (on the left side) and for Simulation 2 (on the right side).

4.2. Sensitivity analysis of soluble species solubility

The model of particle deposition used in Simulation 1 is based on flow phenomena and only depends on hydraulic parameters. This model is by nature not sensitive to chemical parameters such as soluble species solubility. The model of particle deposition coupled with the strengthening process used in Simulation 2 is linked to hydraulic parameters and chemical parameters such as soluble species solubility. Therefore the sensitivity analysis has been only performed for Simulation 2, and more specifically on magnetite solubility. We remember that the magnetite solubility represents the maximum mass fraction of magnetite which is possible to dissolve in liquid.

Four deposit simulations have been performed over a period of 22 years by decreasing the value of magnetite solubility in the secondary flow of Steam Generator from 5 μg/kg to 2 μg/kg as shown in Fig. 15. In this work, the magnetite solubility of the considered Steam Generator was supposed to be at a very high value during all its working period. Therefore the 5 μg/kg magnetite solubility simulation performed in Section 4.1.2 is the reference simulation for this Steam Generator. In this simulation, the deposit model

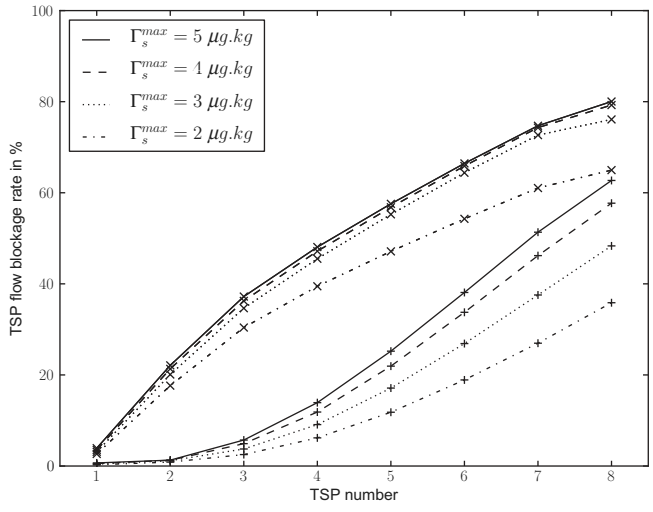

Fig. 15. Sensitivity analysis of magnetite solubility Γ_s^{max} on profiles of mean Tube Support Plate flow blockage rates in hot leg (×) and in cold leg (+).

was adjusted by the inverse method on TV Inspections, and the unobservable parameter was valued at 0.00087. The three other simulations are then performed by taking the magnetite solubility respectively equal to 4 μg/kg, 3 μg/kg and 2 μg/kg. These simulations aim to quantify the impact that such a magnetite solubility decrease would have had on Tube Support Plate flow blockage profiles for the considered Steam Generator. Each of these simulations was thus performed with the same value of the unobservable parameter which is now supposed to be known. In other words, it means that is no calibration was done by the inverse method.

The lower the magnetite solubility is, the more the mean flow blockage rate at each Tube Support Plate decreases. In hot leg, the mean flow blockage rate at the upper Tube Support Plate goes down by 1%, 5% and 20% respectively for the 4 μg/kg, 3 μg/kg and 2 μg/kg magnetite solubility simulations in comparison with the reference simulation. In cold leg, it goes down respectively by 8%, 23% and 43% in comparison with the reference simulation. Therefore a reduction of magnetite solubility in Steam Generators seems to be an interesting remedy for reducing the Tube Support Plate flow blockage phenomenon, and more specifically for Tube Support Plates at the top of Steam Generators. According to the deposit model developed in this work, this reduction would be more effective in cold leg than in hot leg.

In practice, such a magnetite solubility reduction can be obtained by increasing the pH of the secondary circuit. This pH elevation is one of the remedy considered at short term on EDF fleet for its potential benefit on both tube fouling and Tube Support Plate flow blockage. Indeed the operational pH of secondary circuits were planned to raise at certain nuclear plants. This remedy is in agreement with the results obtained in this work.

5. Conclusions

Tube Support Plate flow blockage in nuclear power plants is a concern for EDF and motivates the R&D Division to implement a model for the growth of solid deposits on the secondary side of Steam Generators in the EDF thermal-hydraulic reference code THYC. This model aims to predict the localization and the growth rate of deposits in order to simulate tube fouling, as well as Tube Support Plate flow blockage leading to flow induced vibrations and tube cracks in some cases.

For tube fouling, the deposit model is based on classical mass transfer correlations. For Tube Support Plate flow blockage, mass

transfer correlations based on two main steps have been developed in this work: particle deposition, and strengthening process called "flashing" due to soluble species precipitation in the pores of particle deposit. These correlations depend on an unobservable parameter which can be tuned from the plants experience by an inverse method also developed in this work. This inverse method is able to evaluate a value for this unobservable parameter in Pressurized Water Reactors conditions, by fitting the results of the deposit simulations to the actual levels of Tube Support Plate flow blockage observed in some nuclear plants.

The results obtained in this work underline two dominant trends for the Tube Support Plate flow blockage in Steam Generators: the blockage rate is more important on the hot leg than on the cold leg and at the top than at the bottom of Steam Generators. The blockage rates at the upper Tube Support Plate have the special feature to be more important at the periphery than at the center. The "flashing" phenomenon allows one to underline the magnetite solubility dependence, so the pH dependence, of Tube Support Plate flow blockage phenomenon. A pH elevation of the secondary circuit seems to be an interesting remedy which is currently considered on EDF fleet.

One of the limits of the model in comparison to TV Inspections is that the obtained distributions are necessarily symmetrical at each Tube Support Plate. Two suggestions could be help to solve this problem. Firstly some tubes are plugged during the Steam Generator working. Taking into account of plugging would have an non-symmetrical impact on thermal-hydraulics, and so on deposition. Secondly the swirl imparted by the separators could also induce a non symmetrical distribution of transported particles and solubles species all over the Steam Generators. The mass fraction distribution, and so deposition, would be affected by such a change.

Future work could be performed on several points. Firstly the inverse method could be extended to a more sophisticated inverse method. For instance some methods are available in order to create parametric models (Walter and Pronzato, 1994). Secondly the deposit model could be enhanced by taking into account other deposit mechanisms. Another mechanism than "flashing" which could explain Tube Support Plate flow blockage is called the electrokinetic phenomenon (Robertson, 1986). This phenomenon could induce the formation of deposits at the inlet of flow holes due to the presence of streaming current loops in the immediate vicinity of surface singularities (Guillodo et al., 2004; Barale et al., 2008; Turner and Klimas, 2008). Efforts could be performed in order to implement an electrokinetic mechanism in the model. Moreover the mechanism of deposit removal which is neglected in this work could be also developed and implemented in the model. Thirdly no impact of Tube Support Plate flow blockage on thermal-hydraulic flows has been taken into account in this work. Yet flow blockage causes high velocity zones and transverse velocities in Steam Generators. These impacts could be quantify by performing a coupling between the deposit model and the thermal-hydraulic code.

References

Archambeau, F., Méchitoua, N., Sakiz, M., 2004. A finite volume code for the computation of turbulent incompressible flows – industrial applications. Int. J. Finite Vol. 1.

Barale, M., Guillodo, M., Long, A., Foucault, M., 2008. Étude de l'encrassement des GV au travers des mesures de potentiel zêta. AREVA NP (NTCC-F R 07-1302).

Beal, S.K., Chen, J.H., 1986. A Model of Sludge Behavior in Nuclear Plant Steam Generators. Electric Power Research Institute (NP-4620).

Brunin, O., Deotto, G., David, F., Pillet, J., Dague, G., Nicili, A., 2010. Measurement of pressure loss throughout a clogged steam generator tube support plate in single phase flow. In: ASME Pressure Vessels and Piping Division Conference (PVP2010-25606), Bellevue, Washington, July.

Corredera, G., Alves-Vieira, M., De Bouvier, O., 2008. Fouling and TSP blockage of steam generators on EDF fleet: identified correlations with secondary water chemistry and planned remedies. In: International Conference on Water Chemistry of Nuclear Reactor Systems, Berlin, September.

David, F., 1999. Three dimensional thermal-hydraulic simulation in steam generators with THYC exchangers code: application to the USTG model 73/19. In: Ninth International Topical Meeting on Nuclear Reactor Thermal Hydraulics (NURETH-9), San Francisco, California, October.

Demasles, H., Mercier, P., Tochon, P., 2006. Étude bibliographique sur l'encrassement des échangeurs de chaleur. CEA (DTS/DR/2006/38).

EPRI, 2007. Steam ATHOS/SGAP 3-1, Analysis of Thermal Hydraulics of Steam Generators/Steam Generator Analysis Package, Version 3.1. Mathematical and Physical Models and Method of Solution (1016564).

Guillodo, M., Combrade, P., Dos Santos, B., Muller, T., Berthollon, G., Engler, N., Brun, C., Turluer, G., 2004. Formation of deposits in HT water under high velocity conditions: a parametric study. In: International Conference of Water Chemistry of Nuclear Reactor Systems, San Francisco, California, October.

Klimas, S., Turner, C., 2009. Flow Blockage of Trefoil and Quatrefoil Tube Support Structures in Nuclear Steam Generators. Atomic Energy of Canada Limited (Global Nuclear Products 33110-ASD-001).

Liner, Y., Carver, M.B., Campagna, A.O., 1990. Mathematical modelling of material transport and sludge formation in nuclear steam generators. In: Steam Generator and Heat Exchanger Conference 1, Toronto, April.

Liner, Y., Carver, M.B., Turner, C.W., Campagna, A.O., 1992. Simulation of Magnetite Particulate Fouling in Nuclear Steam Generators, vol. 8. American Society of Mechanical Engineers.

Moleiro, E., Oukacine, F., Adobes, A., 2010. Secondary fouling and tube support plate flow blockage: a model based on transport equations. In: International Conference on Steam Generator Management Program, San Antonio, March.

Pascal-Ribot, S., Debec-Mathet, E., Grandotto, M., Obry, P., 1997. Sludge deposit simulation with the 3D code GENEPI. In: 5th International Conference on Nuclear Engineering, Nice, France, May.

Prusek, T., Moleiro, E., Oukacine, F., Touazi, O., Adobes, A., 2011. Tube fouling and tube support plate blockage in steam generators: inverse method for the estimation of unobservable parameters in a deposit model. In: 19th International Conference on Nuclear Engineering (ICONE-19), Osaka University, Japan, October.

Prusek, T., Moleiro, E., Oukacine, F., Touazi, O., Grandotto, M., Jaeger, M., Adobes, A., 2011. Deposit model for tube support plate flow blockage in steam generators. In: 14th International Topical Meeting on Nuclear Reactor Thermal Hydraulics (NURETH-14), Toronto, September.

Pujet, S., Rodet, I., Dijoux, M., 2004. Modeling of the combined effects of particle deposition and soluble iron precipitation on PWR steam generator fouling. In: International Conference on Water Chemistry of Nuclear Reactor Systems, San Francisco, California, October.

Robertson, J., 1986. Corrosion and Deposition Due to Electrokinetic Currents. Central Electricity Research Laboratories (TPRD/L/3030/R86 00079).

Rummens, H.E.C., Rogers, J.T., Turner, C.W., 2004. The thermal hydraulics of tube support fouling in nuclear steam generators. Nucl. Technol., 148.

Rummens, H.E.C., 1999. The Thermal Hydraulics of Tube-Support Fouling in Nuclear Steam Generators. Carleton University, Ontario, Canada (PhD Thesis).

Tarantola, A., 1994. Inverse Problem Theory: Methods for Data Fitting and Model Parameter Estimation. Elsevier, Amsterdam, The Netherlands.

Turner, C.W., Klimas, S., 2008. Fouling of Tube Support Plates – Knowledge Gaps. Atomic Energy of Canada Limited (Global Nuclear Products 33110-440-001).

Turner, C.W., Liner, Y., Carver, M.B., 1994. Modelling magnetite particle deposition in nuclear steam generators and comparisons with plant data. In: 2nd Conference on Steam Generators and Heat Exchangers 1–2, Toronto, June.

Varrin, R., 2010. Characterization on PWR Steam Generator Deposits. Electric Power Research Institute (TR-106048).

Walter, E., Pronzato, L., 1994. Identification de modèles paramétriques. Masson, Paris, France.